K-Nearest Neighbors Gaussian Process Regression for Urban Radio Map Reconstruction

Yifang Zhang and Shaowei Wang

***Abstract*—Radio map is of great importance to interference control, network planning and resource allocation in wireless communications. In this paper, we develop an accurate radio map reconstruction method based on k-nearest neighbors Gaussian process regression, which can exploit the relationship of the received signal strengths at adjacent locations efficiently. Numerical experiments demonstrate that our proposed method outperforms the state-of-the-art ones significantly.**

***Index Terms*—Gaussian process regression, k-nearest neighbors, radio map reconstruction.**

I. Introduction

RADIO map is an effective performance indicator of wireless network. Reconstructing the precise radio map of a wireless network is the cornerstone of numerous applications such as resource allocation, interference control, fingerprint based localization and network planning [1]. Moreover, as the advances of 5G and beyond mobile communications, it is particularly necessary to maintain a fine-grained radio map to effectively utilize the limited radio spectrum resource, as well as power and energy.

Generally speaking, a radio map can be expressed in terms of Received Signal Strength (RSS), which may be affected by different factors, such as distance-dependent propagation loss, reflection and diffraction from buildings, random shadowing and small-scale fading, especially in urban environments [2]. To cope with such a complex scenario, a variety of model-based approaches for estimating the radio map have been proposed, including the empirical models [3], the ray-tracing models [4] and the dominant path models [5]. Empirical models are usually simple and easy to use but cannot adapt to variable environments. The prediction accuracy of the ray-tracing model is high due to the detailed input parameters, however, the huge computation overhead prohibits it from applications in a large area and complex environment, which is always the case in practical scenarios. Dominant path models only focus on the dominant ray path between the transmitter and receiver, which reduce the computation time but also result in lower prediction accuracy.

A common drawback of the aforementioned model-based methods is that the RSS measurements reported by terminals are not leveraged fully. It would be of great help if the RSS measurements as well as location information reported by user terminals can be exploited to reconstruct the radio map of the target wireless network. Consequently, data driven methods have gained attention recently. Different from the model-based estimation, complex environment information such as building height and terrain height is not required in data driven methods. Instead, a finite set of RSS measurements known at certain locations is utilized to estimate the RSSs at non-measured locations via interpolation approaches including Kriging [6], Radial Basis Functions (RBF) [7], matrix completion [8] and Kernel Ridge Regression (KRR) [9]. As far as the authors have known, these methods exploit the spatial correlation of the radio map and can work well in unobstructed environments where radio maps exhibit spatial smooth patterns. However, in practice, large buildings and obstacles in urban environments can abruptly attenuate electromagnetic waves, which means that radio maps show spatial correlation and smoothness only in local areas in urban environments.

Against this background, we propose a k-nearest neighbors Gaussian Process Regression (GPR) method, referred to as K-GP, to reconstruct the radio map in urban environments. The GPR is a powerful approach to model and exploit unknown functions [10], which performs well in various areas such as robot localization [11], indoor positioning [12] and motion trajectory prediction [13]. In [11], path loss models and GPR are incorporated to generate indoor radio mappings. However, target areas in urban environments are usually larger than in indoor ones, making it computationally expensive to construct an urban radio map through GPR. Also, a single set of hyper-parameters is used and optimized for all points, which reduces the prediction accuracy. In our proposed method, we apply the GPR to the neighborhood of each estimation point instead of taking all the measured points in target region as training data to capture the local characteristics of urban radio map. Also, the appropriate number of neighbor points under different sampling percentages are investigated. Further, different sets of hyper-parameters are used and optimized for each estimated point. Therefore, for every estimation point, the underlying characteristics in surrounding RSS distribution are exploited individually. Additionally, the computational complexity of our proposed K-GP scales only linearly with the number of non-measured points, which is acceptable in practical applications. Numerical experiments show that our proposed algorithm achieves notable prediction accuracy advantage.

The rest of this paper is organized as follows. In Section II, we formulate the prediction problem. Section III describes the K-GP method in detail. Experiment results and discussions

Manuscript received June 27, 2022; revised August 11, 2022 and September 8, 2022; accepted September 9, 2022. This work was partially supported by the National Natural Science Foundation of China under Grants 61931023 and U1936202. The associate editor coordinating the review of this letter and approving it for publication was A. Guerra. *(Corresponding author: Shaowei Wang.)*

The authors are with the School of Electronic Science and Engineering, Nanjing University, Nanjing 210023, China (e-mail: mg21230076@smail.nju.edu.cn, wangsw@nju.edu.cn).

are reported in Section IV. Section V concludes this paper.

II. Problem Formulation

Consider a certain region of interest served by a set $\mathcal{B} = \{1, \cdots, B\}$ of base stations. Without loss of generality, we assume that the region is divided into $P = N_x \times N_y$ rectangular grids with the size of small grid δ_x along the x-axes and δ_y along the y-axes. Denote the set of grid points by $\mathcal{G} = \{\boldsymbol{x}_p\}_{p=1}^{P}$, where $\boldsymbol{x}_p$ is a two-dimensional coordinate. We consider a base station $b \in \mathcal{B}$, devices such as smart phones periodically send their location information as well as the RSS measurements to the base station b, which can be stored and utilized for radio map reconstruction. Let $R(\boldsymbol{\varphi}_i)$ denote the RSS measurement at location $\boldsymbol{\varphi}_i$. Note that $\boldsymbol{\varphi}_i$ may not be exactly on the grid point, and some of the measured locations may fall into the same grid.

To deal with such situation, we define $\mathcal{C}_p$ as the set of the measured locations assigned to the grid point $\boldsymbol{x}_p$ according to the minimum distance criterion [14]. More specifically, $\boldsymbol{\varphi}_i \in \mathcal{C}_p$ if the following inequality is satisfied:

$$\| \boldsymbol{x}_p - \boldsymbol{\varphi}_i \| \leq \| \boldsymbol{x}_{p'} - \boldsymbol{\varphi}_i \| , \forall \boldsymbol{x}_{p'} \in \mathcal{G}. \tag{1}$$

When $|\mathcal{C}_p| > 0$, the RSS of the grid point $R(\boldsymbol{x}_p)$ can be approximated by

$$R(\boldsymbol{x}_p) = \frac{1}{|\mathcal{C}_p|} \sum_{i \in \mathcal{C}_p} R(\boldsymbol{\varphi}_i). \tag{2}$$

When $|\mathcal{C}_p| = 0$, it indicates that the grid point $\boldsymbol{x}_p$ has no RSS measurements assigned to it and we call such point a non-measured point. Compared to the continuous radio map, dividing the map into grids has advantages such as averaging the uncertainty of collected location information caused by location drifts and reducing the noise of RSS measurements by taking the average of measurements within a grid.

Let $\boldsymbol{X}$ be the set of grid points $\boldsymbol{x}_n$ such that $|\mathcal{C}_n| > 0$ and $\boldsymbol{X}^*$ be the set of grid points $\boldsymbol{x}_m$ such that $|\mathcal{C}_m| = 0$. Denote by N the number of measured points and M the number of non-measured points. The RSS measurement of grid point $\boldsymbol{x}_n$ is denoted by $R(\boldsymbol{x}_n)$ and the set of all measured points is denoted by $\boldsymbol{R}$. Similarly, we denote $R^*(\boldsymbol{x}_m)$ the RSS value at non-measured point $\boldsymbol{x}_m$ and $\boldsymbol{R}^*$ the set of RSS values of all non-measured points. The problem to solve is to estimate the RSS values $\boldsymbol{R}^*$ at non-measured points $\boldsymbol{X}^*$ given measurements $\boldsymbol{R}$ and location information $\boldsymbol{X}$.

III. Radio Map Reconstruction Algorithm

GPR is an efficient nonparametric and nonlinear approach which can capture the noisy nature of RSS and is suitable to depict the RSS function property in real world. For the considered radio map reconstruction problem, RSS measurements and the corresponding locations can be modeled as a Gaussian process, that is

$$R = f(\boldsymbol{x}) + \varepsilon, \tag{3}$$

where $\boldsymbol{x}$ is the two-dimensional coordinate of a measured point, R is the measured RSS at location $\boldsymbol{x}$, $f(\boldsymbol{x})$ denotes the true RSS at location $\boldsymbol{x}$, and ε denotes an addictive zero-mean Gaussian noise with variance σ_n^2. Assume the RSS measurements at measured locations can be drawn from a Gaussian process

$$R \sim \mathcal{GP}(m(\boldsymbol{x}), k(\boldsymbol{x}, \boldsymbol{x}')), \tag{4}$$

where $m(\boldsymbol{x})$ denotes the mean function and $k(\boldsymbol{x}, \boldsymbol{x}')$ denotes the covariance function of Gaussian process. To reduce computational complexity, the covariance function in Gaussian process is presented by the kernel function. Notice that the kernel function indicates the correlation between two points, in general, the closer the Euclidean distance between two points is, the more likely their RSSs are similar. To this end, we choose the RBF kernel [15] to represent the covariance function which is expressed as

$$k(\boldsymbol{x}, \boldsymbol{x}') = \sigma_f^2 exp(-\frac{1}{2\beta^2} \|\boldsymbol{x} - \boldsymbol{x}'\|^2), \tag{5}$$

where σ_f^2 and β are the hyper-parameters of Gaussian process. In conventional Gaussian process, the covariance of each pair of measured points is calculated according to (5) and an $N \times N$ covariance matrix $K(\boldsymbol{X}, \boldsymbol{X})$ for all pairs of measured points is obtained, which is given by

$$K = \begin{bmatrix} k_{11} & k_{12} & \cdots & k_{1N} \\ k_{21} & k_{22} & \cdots & k_{2N} \\ \vdots & \vdots & \ddots & \vdots \\ k_{N1} & k_{N2} & \cdots & k_{NN} \end{bmatrix} \tag{6}$$

We would like to predict RSS values $\boldsymbol{R}^*$ at locations $\boldsymbol{X}^*$. The marginalization feature of Gaussian process enables us to calculate the posterior probability at unknown input $\boldsymbol{X}^*$ if some observations are available at the given inputs $\boldsymbol{X}$. The unknown RSS values of $\boldsymbol{X}^*$ and RSS measurements of $\boldsymbol{X}$ satisfy a joint Gaussian distribution, i.e.

$$\begin{bmatrix} \boldsymbol{R} \\ \boldsymbol{R}^* \end{bmatrix} \sim \mathcal{N}\left(\begin{bmatrix} \boldsymbol{\mu} \\ \boldsymbol{\mu}^* \end{bmatrix}, \begin{bmatrix} K(\boldsymbol{X}, \boldsymbol{X}) + \sigma_n^2 I & K(\boldsymbol{X}, \boldsymbol{X}^*) \\ K(\boldsymbol{X}^*, \boldsymbol{X}) & K(\boldsymbol{X}^*, \boldsymbol{X}^*) \end{bmatrix} \right), \tag{7}$$

where $K(\boldsymbol{X}^*, \boldsymbol{X})$ and $K(\boldsymbol{X}, \boldsymbol{X}^*)$ are $M \times N$ and $N \times M$ matrices of the covariance between points $\boldsymbol{X}^*$ and $\boldsymbol{X}$, $K(\boldsymbol{X}, \boldsymbol{X})$ is an $N \times N$ covariance matrix, I is the identical matrix. $\boldsymbol{\mu} = m(\boldsymbol{x}_n), n = 1, \cdots, N$ are the RSS means of measured points and $\boldsymbol{\mu}^*$ are the RSS means of non-measured points. $\boldsymbol{\mu}$ and $\boldsymbol{\mu}^*$ are all set to $\frac{1}{N}\sum_{n=1}^{N} R(\boldsymbol{x}_n)$. The predicted RSS values for interested points $\boldsymbol{X}^*$ can be obtained according to the posterior mean and covariance of Gaussian process

$$p(\boldsymbol{R}^* | \boldsymbol{X}, \boldsymbol{R}, \boldsymbol{X}^*) \sim N(\boldsymbol{u}_*, \boldsymbol{\Sigma}_*), \tag{8}$$

$$\boldsymbol{u}_* = \boldsymbol{\mu}^* + K(\boldsymbol{X}^*, \boldsymbol{X})[K(\boldsymbol{X}, \boldsymbol{X}) + \sigma_n^2 I]^{-1}(\boldsymbol{R} - \boldsymbol{\mu}), \tag{9}$$

$$\begin{aligned} \boldsymbol{\Sigma}_* = &- K(\boldsymbol{X}^*, \boldsymbol{X})[K(\boldsymbol{X}, \boldsymbol{X}) + \sigma_n^2 I]^{-1} K(\boldsymbol{X}, \boldsymbol{X}^*) \\ &+ K(\boldsymbol{X}^*, \boldsymbol{X}^*), \end{aligned} \tag{10}$$

where $\boldsymbol{u}_*$ is an $M \times 1$ vector which indicates the estimated mean RSS values at location $\boldsymbol{X}^*$, $\boldsymbol{\Sigma_*}$ is an $M \times M$ matrix whose diagonal elements indicate the estimation confidence.

Observe that in (9), the inversion of matrix $K(\boldsymbol{X}, \boldsymbol{X}) + \sigma_n^2 I$ needs to be calculated, which yields a complexity of $O(N^3)$

This article has been accepted for publication in IEEE Communications Letters. This is the author's version which has not been fully edited and content may change prior to final publication. Citation information: DOI 10.1109/LCOMM.2022.3207210

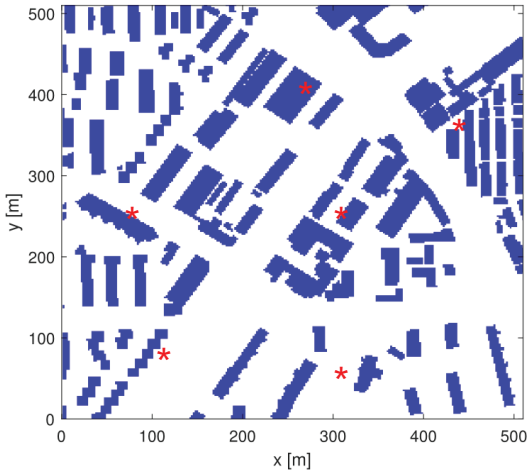

Fig. 1: The deployment of the BSs where the BSs are marked in red star.

and leads the training of GPR to suffer from heavy computation load when N is large. Moreover, taking all measured points into account may also reduce the accuracy of prediction since the RSSs of the points over large distances are totally unrelated. Actually, a more accurate RSS prediction of non-measured point can be achieved by considering only the local neighborhood.

To this end, we present a K-GP method to estimate the RSS of an individual point $\boldsymbol{x}^*$. Let L denote the number of the nearest neighbors of the estimated point. According to k-nearest neighbors algorithm, define $\tilde{\boldsymbol{X}} = \{\boldsymbol{x}_l\}_{l=1}^{L}$ as the set containing the location of L closest points to the point $\boldsymbol{x}^*$ and $\tilde{\boldsymbol{R}} = \{R(\boldsymbol{x}_l)\}_{l=1}^{L}$ as the RSS measurements accordingly. Then the training data in GPR is $\{(\boldsymbol{x}_l, R(\boldsymbol{x}_l))\}_{l=1}^{L}$ instead of the whole set of measured points. More specifically, if we want to calculate the estimated RSS value R^* of $\boldsymbol{x}^*$, the joint Gaussian distribution described in (7) can be rewritten as follows:

$$\begin{bmatrix} \tilde{\boldsymbol{R}} \\ R^* \end{bmatrix} \sim \mathcal{N}\left(\begin{bmatrix} \tilde{\boldsymbol{\mu}} \\ \mu^* \end{bmatrix}, \begin{bmatrix} K(\tilde{\boldsymbol{X}}, \tilde{\boldsymbol{X}}) + \sigma_n^2 I & K(\tilde{\boldsymbol{X}}, \boldsymbol{x}^*) \\ K(\boldsymbol{x}^*, \tilde{\boldsymbol{X}}) & K(\boldsymbol{x}^*, \boldsymbol{x}^*) \end{bmatrix} \right), \tag{11}$$

where $K(\boldsymbol{x}^*, \tilde{\boldsymbol{X}})$ and $K(\tilde{\boldsymbol{X}}, \boldsymbol{x}^*)$ are $1 \times L$ and $L \times 1$ matrices, $K(\tilde{\boldsymbol{X}}, \tilde{\boldsymbol{X}})$ is an $L \times L$ covariance matrix. Similarly, the predicted RSS of $\boldsymbol{x}^*$ can be obtained by

$$p(R^* | \tilde{\boldsymbol{X}}, \tilde{\boldsymbol{R}}, \boldsymbol{x}^*) \sim N(u_*, \sigma_*^2), \tag{12}$$

$$u_* = \mu^* + K(\boldsymbol{x}^*, \tilde{\boldsymbol{X}})[K(\tilde{\boldsymbol{X}}, \tilde{\boldsymbol{X}}) + \sigma_n^2 I]^{-1}(\tilde{\boldsymbol{R}} - \tilde{\boldsymbol{\mu}}), \tag{13}$$

$$\sigma_*^2 = K(\boldsymbol{x}^*, \boldsymbol{x}^*) - K(\boldsymbol{x}^*, \tilde{\boldsymbol{X}})[K(\tilde{\boldsymbol{X}}, \tilde{\boldsymbol{X}}) + \sigma_n^2 I]^{-1} K(\tilde{\boldsymbol{X}}, \boldsymbol{x}^*), \tag{14}$$

where u_* is taken as the estimated RSS value at location $\boldsymbol{x}^*$. Since L is a constant, the computational complexity of K-GP is $O(M)$, which is much smaller than $O(N^3)$.

The hyper-parameters $\theta = \{\sigma_f, \beta\}$ can be obtained by optimizing the following log marginal likelihood function:

$$\begin{aligned} &\log p(\tilde{\boldsymbol{R}} | \tilde{\boldsymbol{X}}, \theta) \\ &= -\frac{1}{2}(\tilde{\boldsymbol{R}} - \tilde{\boldsymbol{\mu}})^\top (K(\tilde{\boldsymbol{X}}, \tilde{\boldsymbol{X}}) + \sigma_n^2 I)^{-1}(\tilde{\boldsymbol{R}} - \tilde{\boldsymbol{\mu}}) \\ &- \frac{1}{2}\log\left| K(\tilde{\boldsymbol{X}}, \tilde{\boldsymbol{X}}) + \sigma_n^2 I \right| - \frac{Q}{2}\log(2\pi), \end{aligned} \tag{15}$$

where the optimal $\theta = \{\sigma_f, \beta\}$ can be worked out based on the partial derivatives of (15) as follows:

$$\begin{aligned} \frac{\partial \log p(\tilde{\boldsymbol{R}} | \tilde{\boldsymbol{X}}, \theta)}{\partial \theta_i} &= \frac{1}{2} trace(K(\tilde{\boldsymbol{R}}, \tilde{\boldsymbol{R}})^{-1} \frac{\partial K(\tilde{\boldsymbol{R}}, \tilde{\boldsymbol{R}})}{\partial \theta_i}) \\ &+ \frac{1}{2}(\tilde{\boldsymbol{R}} - \tilde{\boldsymbol{\mu}})^\top \frac{\partial K(\tilde{\boldsymbol{R}}, \tilde{\boldsymbol{R}})}{\partial \theta_i} K(\tilde{\boldsymbol{R}}, \tilde{\boldsymbol{R}})^{-1} \frac{\partial K(\tilde{\boldsymbol{R}}, \tilde{\boldsymbol{R}})}{\partial \theta_i}(\tilde{\boldsymbol{R}} - \tilde{\boldsymbol{\mu}}). \end{aligned} \tag{16}$$

Gradient descent methods can be employed to solve (16). Since every estimated point has its unique neighbor points, the hyper-parameters are adjusted specifically for each point instead of using a single set of parameters for all points.

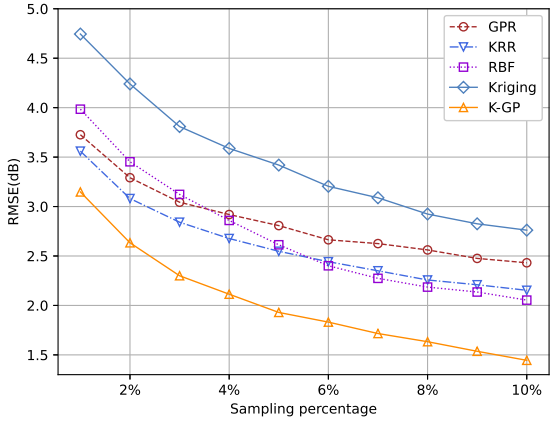

(a) 3.5 GHz

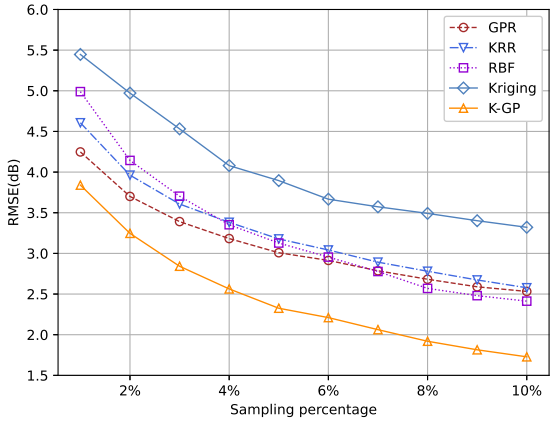

(b) 30 GHz

Fig. 2: RMSE as a function of the sampling percentage.

This article has been accepted for publication in IEEE Communications Letters. This is the author's version which has not been fully edited and content may change prior to final publication. Citation information: DOI 10.1109/LCOMM.2022.3207210

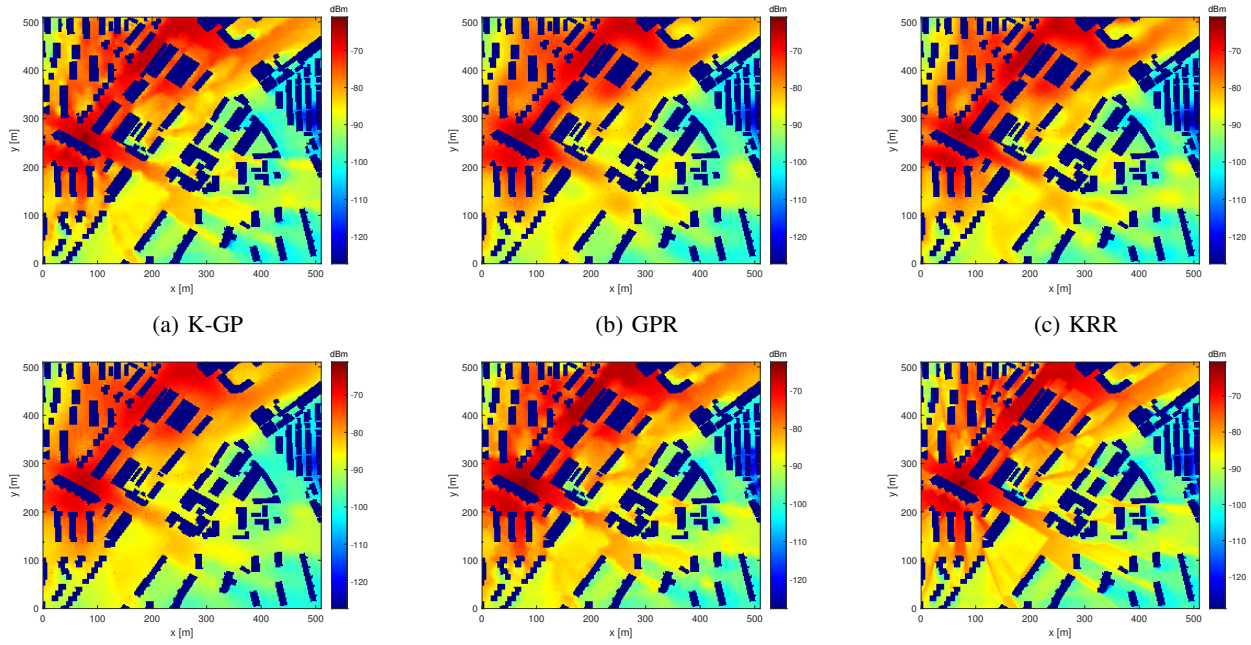

(a) K-GP (b) GPR (c) KRR

(d) Kriging (e) RBF (f) True RSS distribution

Fig. 3: The reconstructed radio maps through different methods and the true RSS distribution.

IV. Numerical Experiments

We evaluate the proposed K-GP method in an urban environment, where the true RSS distributions are generated by 3D intelligent ray tracing model [16] with Maxwell's equations. 30 city maps in different locations as well as different base station locations are generated. The city maps are taken from a metropolis and the heights of buildings are set to their actual values. The height of receivers and transmitters is set to 1.5m and 40m, respectively. The locations of transmitters are modeled by a Poisson point process and Fig. 1 shows an example of the locations of BSs. The radio frequency is set to 3.5 GHz while the transmit power is set to 23 dBm. In addition, the target region is a square area of $512 \times 512m^2$, which is divided into grids with $N_x \times N_y = 256 \times 256$. The measured locations are drawn randomly over the target region.

To test the performance of the K-GP method under different percentage of RSS measurements, we set the sampling percentage S from 1% to 10%. More specifically, the number of measurements is about 500 when the sampling percentage equals 1%. Next, we compare our proposed method with other methods: the Kriging [6], the RBF [7], the KRR [9] and the traditional GPR. We adopt Root Mean Square Error (RMSE) as the performance metric, which is defined as follows,

$$\mathrm{RMSE} = \sqrt{\frac{\sum_{\mathrm{m}=1}^{\mathrm{M}} (\breve{\mathrm{R}}(\boldsymbol{x}_{\mathrm{m}}) - \mathrm{R}^*(\boldsymbol{x}_{\mathrm{m}}))^2}{\mathrm{M}}}, \qquad (17)$$

where $\breve{R}(\boldsymbol{x}_m)$ and $R^*(\boldsymbol{x}_m)$ denote the true RSS value and estimated RSS one at point $\boldsymbol{x}_m$, respectively.

Fig. 2 shows the average RMSE as a function of the percentage of sampling points when $L = 6$. When the radio frequency is set to 3.5 GHz and 30 GHz, it can be seen that as the sampling percentage increases, the RMSE decreases for all

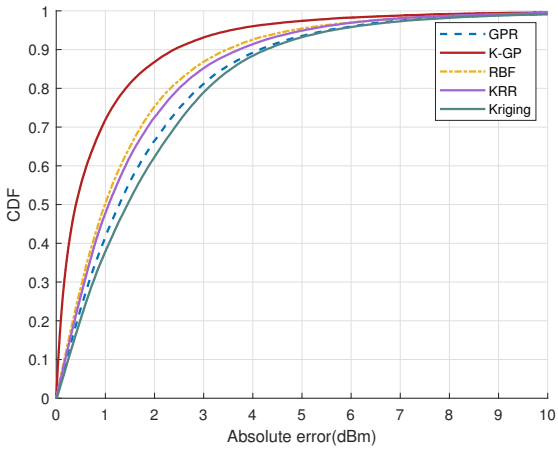

Fig. 4: CDF of the absolute error.

methods and the K-GP method outperforms the others significantly. The K-GP method reaches better prediction accuracy than the GPR method because the K-GP method ignores the unnecessary effect of distant measured points. Observe that with just sampling percentage $S = 5\%$, the reconstructed radio map of the K-GP method is already of a high quality. When the sampling percentage is as high as 10%, the RMSE of our proposed method can be as low as 1.4 dB.

To present the experimental results more intuitively, the radio reconstruction results through different methods under a special case of BS distributions are shown in Fig. 3. The radio frequency is set to 3.5 GHz and the sampling percentage is 7%. Compared with other methods, more details in the radio map can be obtained by the K-GP. The abrupt change of RSSs caused by obstructions can be captured by the K-

This article has been accepted for publication in IEEE Communications Letters. This is the author's version which has not been fully edited and content may change prior to final publication. Citation information: DOI 10.1109/LCOMM.2022.3207210

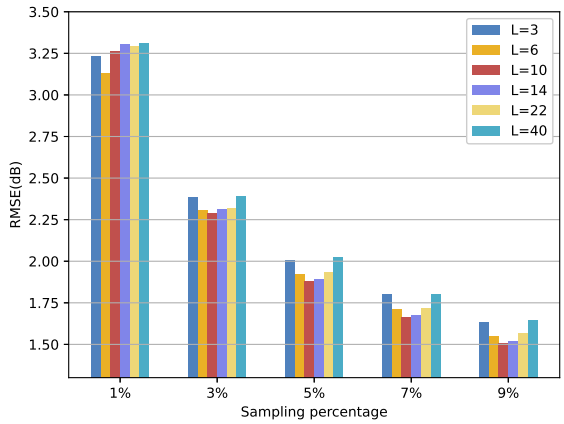

Fig. 5: RMSE of prediction with varying number of neighbors.

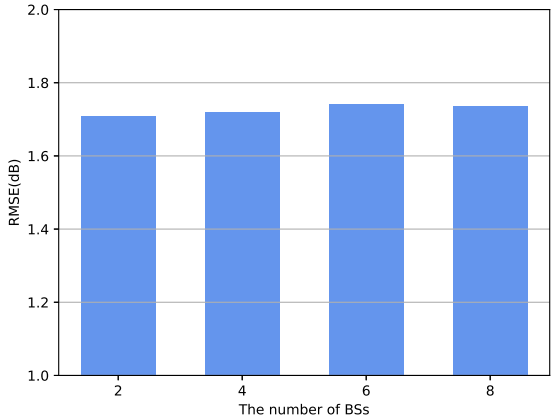

Fig. 6: RMSE of K-GP as a function of the number of BSs.

GP while such details are neglected by other methods. This can be explained as follows: For each estimation point, the mean value and hyper-parameters of the K-GP are adjusted according to the nearby RSS measurements which reflect the local characteristics of the surrounding area. Additionally, the corresponding CDF of the absolute error is shown in Fig. 4, indicating that the K-GP method achieves the best performance and about 90% of the estimated points has an absolute error less than 2.5 dBm.

Furthermore, we discuss the influence of the number of neighbors on the prediction accuracy. Fig. 5 depicts the RMSE of prediction with varying number of neighbors. The results show that when sampling percentage equals 1%, K-GP with $L = 6$ neighbors reaches the best prediction accuracy. The reason is that the measured points are far from each other, fewer neighbors can better represent local characteristics. In other sampling percentages such as $3\%, 5\%, 7\%, 9\%$, the K-GP with $L = 10$ neighbors yields the best performance. Additionally, the effect of the number of BSs has also been investigated. When the sampling percentage is 7% and $L = 10$, the RMSE result of our proposed method under different number of base stations is shown in Fig. 6. It can be seen that with different number of base stations, the RMSE of the K-GP method keeps stable around 1.7 dB, which shows the robustness of the method.

V. Conclusion

In this paper, we have presented a novel interpolation method for reconstructing urban radio maps with a given set of RSS measurements. A Gaussian process regression is employed to estimate the RSSs of non-measured points with their k-nearest neighbors, which can significantly reduce the computational complexity of the Gaussian process regression. The performance of our proposed method is evaluated in an urban environment and significant accuracy improvements can be found from the experimental results. For future work, we may investigate the effect of the heights of transmitters and receivers. Besides, the performance of the proposed method in a realistic measured data set will also be evaluated.

References

[1] T. V. Chien *et al.*, "Power control in cellular massive mimo with varying user activity: A deep learning solution," *IEEE Trans. Wirel. Commun.*, vol. 19, no. 9, pp. 5732–5748, Sept. 2020.

[2] R. Levie *et al.*, "RadioUNet: fast radio map estimation with convolutional neural networks," *IEEE Trans. Wirel. Commun.*, vol. 20, no. 6, pp. 4001–4015, Jun. 2021.

[3] M. F. Iskander and Z. Yun, "Propagation prediction models for wireless communication systems," *IEEE Trans. Microw. Theory. Tech.*, vol. 50, no. 3, pp. 662–673, Mar. 2002.

[4] N. Suga *et al.*, "Ray tracing acceleration using total variation norm minimization for radio map simulation," *IEEE Wirel. Commun. Lett.*, vol. 10, no. 3, pp. 522–526, Mar. 2021.

[5] R. Wahl *et al.*, "Dominant path prediction model for urban scenarios," in *Proc. IST MWC*, Dresden, Germany, Jun. 2005.

[6] G. Boccolini, G. Hernndez-Pealoza, and B. Beferull-Lozano, "Wireless sensor network for spectrum cartography based on Kriging interpolation," in *Proc. IEEE PIMRC*, Sydney, Australia, Nov. 2012.

[7] M. Hamid and B. Beferull-Lozano, "Non-parametric spectrum cartography using adaptive radial basis functions," in *Proc. IEEE ICASSP*, New Orleans, LA, USA, Mar. 2017.

[8] S. Chouvardas *et al.*, "A method to reconstruct coverage loss maps based on matrix completion and adaptive sampling," in *Proc. IEEE ICASSP*, Shanghai, China, Mar. 2016.

[9] S. An, W. Liu, and S. Venkatesh, "Face recognition using kernel ridge regression," in *Proc. IEEE CVPR*, Minneapolis, USA, Jun. 2007.

[10] S. Wang and H. Gu, "Multiuser detection with sparse spectrum Gaussian process regression," *IEEE Commun. Lett.*, vol. 16, no. 2, pp. 164–167, Feb. 2012.

[11] R. Miyagusuku, A. Yamashita, and H. Asama, "Precise and accurate wireless signal strength mappings using gaussian processes and path loss models," *Robot. Auton. Syst.*, vol. 103, no. 2, pp. 134–150, May 2018.

[12] H. Zou *et al.*, "WinIPS: WiFi-based non-intrusive indoor positioning system with online radio map construction and adaptation," *IEEE Trans. Wirel. Commun.*, vol. 16, no. 12, pp. 8118–8130, Dec. 2017.

[13] K. Kim, D. Lee, and I. Essa, "Gaussian process regression flow for analysis of motion trajectories," in *Proc. IEEE ICCV*, Barcelona, Spain, Nov. 2011.

[14] Y. Teganya and D. Romero, "Deep completion autoencoders for radio map estimation," *IEEE Trans. Wirel. Commun.*, vol. 21, no. 3, pp. 1710–1724, Mar. 2021.

[15] B.-C. Kuo *et al.*, "A kernel-based feature selection method for SVM with RBF kernel for hyperspectral image classification," *IEEE J. Sel. Topics Appl. Earth Observ. Remote Sens.*, vol. 7, no. 1, pp. 317–326, Jan. 2014.

[16] R. Hoppe, G. Wlfle, and U. Jakobus, "Wave propagation and radio network planning software WinProp added to the electromagnetic solver package FEKO," in *Proc. ACES*, Florence, Italy, Mar. 2017.